

Response to reviewers comments for:  
“A new diagnostic for tropospheric ozone production”  
(acp-2017-378)

The reviewers comments have been addressed. Below are the authors responses (red) and changes implemented (blue). The reviewers comments (black) have been numbered to avoid confusion.

**Anonymous Referee #1**

This paper presents a novel analysis of ozone production in terms on the spin states of the bonds in the precursor species. This is an interesting and original concept, and is a commendable attempt to generate a diagnostic of ozone production that has a sound physico-chemical basis, and one that provides more process insight than the standard methods based on NO<sub>x</sub> cycling. The paper is worthy of publication, but needs revision to address a number of weaknesses and to enhance its value to the scientific community.

General Comments

1. The background theory behind the diagnostic could be presented more clearly. While the concept of electron spin is well understood in the physical chemistry community, it is necessary to provide a brief introduction for a wider audience, along with references to literature where readers can learn more.

The paragraph in the introduction that introduces spin has been expanded and a reference to an explanation of the fundamental principles included. This paragraph now reads:

The inefficiency of ground state O<sub>2</sub> as an atmospheric oxidant is due to its electronic structure. In quantum mechanics, all atomic particles have an intrinsic angular momentum known as spin [Atkins and De Paula, 2014]. The spin of an electron is described by the spin quantum number, *s*, and can have values of either +½ or -½ for a single electron. The Pauli exclusion principle states that if two electrons occupy the same orbital then their spins must be paired, and thus cancel. With two unpaired electrons ground state O<sub>2</sub> is a spin-triplet with a total spin quantum number  $S=½+½=1$  (giving a term symbol of  ${}^3\Sigma_g^-$ ). In contrast, virtually all trace chemicals emitted into the atmosphere contain only paired electrons and are thus spin-singlets ( $S=0$ ). The quantum mechanical spin selection rule  $\Delta S=0$  means that allowed electronic transitions must not result in a change in electron spin. From a simplistic perspective (i.e. ignoring nuclear spin interactions, inter-system crossings, nuclear dipole effects etc.) this spin selection rule means that the reaction of ground state O<sub>2</sub> with most emitted compounds is effectively spin forbidden. Electronically excited O<sub>2</sub> ( ${}^1\Delta_g$  or  ${}^1\Sigma_g^+$ ) is a spin singlet and is more reactive in the atmosphere but low concentrations limit its role [Larson and Marley, 1999]. Instead, atmospheric oxidation proceeds predominantly via reactions with spin-doublet oxygen-derived species ( $S=½$ ), notably the hydroxyl (OH) and peroxy radicals (RO<sub>2</sub> = HO<sub>2</sub>, CH<sub>3</sub>O<sub>2</sub>, C<sub>2</sub>H<sub>5</sub>O<sub>2</sub>, etc.), or spin-singlet species (e.g. ozone (O<sub>3</sub>)).

2. The paper addresses the rate of ozone production, but discussion focuses solely on long-term integrated ozone production on an annual global scale. It is not clear how applicable the new diagnostic is to smaller regions and shorter timescales where the assumption of steady state (line 141) may be less appropriate, and where emissions may be less important than transport. What is needed to extend the diagnostic to these smaller spatial and temporal scales? The potential for analysis of regional

budgets is alluded to on line 307, but no detail is provided.

The strengths and limitations of the approach should be set out more clearly. What additional insight does the new metric provide and how might this be applied to real problems (e.g., to the sensitivity of ozone production to assumptions of VOC speciation, to simplification of isoprene chemistry, or to treatments of deposition processes?) How does the approach compare with previous attempts to generate diagnostics, e.g., though the concept of photochemical ozone creation potentials (POCPs) for individual VOCs? There is little reference to earlier approaches in the field.

The aim of this paper is to describe a new approach for the study of ozone production in chemical transport models, and to illustrate this through a global budget analysis and comparison with the most commonly used diagnostic for this. The application of the new diagnostic to other scales and problems, as well as comparison to other available metrics is of interest but unfortunately outside the scope of this work. The following paragraph has been added to the conclusion section to discuss the strengths of the approach in relation to other possible applications, and also identify things that would need to be considered for this to be successful.

Future work is necessary to identify the usefulness of this approach on smaller spatial and temporal scales. For regional modelling scale, the transport flux of bonds into the domain would need to be considered alongside the emissions of bonds. However, this might help to disentangle O<sub>3</sub> production due to local VOC emissions from that due to VOC emissions outside of the domain. This bond focussed approach may also have usefulness on shorter timescales. For example, when considering vertical fluxes in and out of the boundary layer, a bond centred approach could help. What fraction of the bonds emitted at the surface are exported to the free troposphere. If a measurement of reactivity flux could be made this could be tested experimentally.

#### Specific Comments

3. Figure 4: please explain how the contributions of the R and F terms presented in the figure are derived. It is easy to see for the standard diagnostic, where the terms sum linearly to the total PO<sub>3</sub>, but it is not as clear for the new diagnostic as the terms are no longer independent of each other (as defined in Eq. 1).

The following text has been added to the figure caption.

The P<sub>s</sub>O<sub>3</sub> diagnostic parameters are derived for each model simulation using the diagnostic implementation described in Sect. 3, and the fractional change in each parameter from the base simulation calculated.

4. The meaning of the horizontal dashed lines in Figure 4 is not clear.

These are gridlines to aid comparison between plots. We have not changed this as we feel it helps interpretation of the figure, but are happy to take the editors guidance.

5. I.270: How many simulations were performed for these sensitivity studies? Please state this in the text.

Text now includes following sentence.

A set of 5 simulations was performed for each model sensitivity investigated ( $\text{NO}_x$ , isoprene and  $\text{CH}_4$ ), with a common base simulation, resulting in 13 simulations in total.

- Figure 7 is not well conceived. It is not clear why a log- $\text{NO}_x$  scale is used, given that the relationships expected are not exponential (neither line drawn here is expected to be straight, as would quickly become evident at larger or smaller  $\text{NO}_x$  levels). Perhaps plot OH vs  $\text{CH}_4$  bond emission directly, and label the points with the  $\text{NO}_x$  level?

We thank the reviewer for this suggestion and have updated the figure to that shown below.

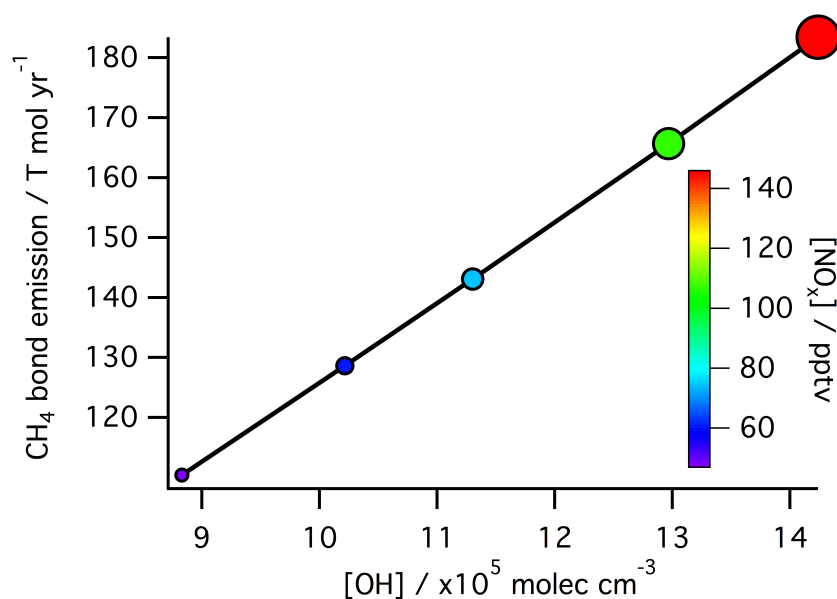


Figure 7. Effective  $\text{CH}_4$  emissions as a function of global mean OH concentration, for simulations where  $\text{NO}_x$  emissions were changed. Marker size and colour indicate global  $\text{NO}_x$  concentration.

- Figures 8 and 10 would be more effectively presented through the use of a bar chart, so that the relative changes can be seen more clearly.

We again thank the reviewer for this suggestion and have remade the figures as bar charts (see below).

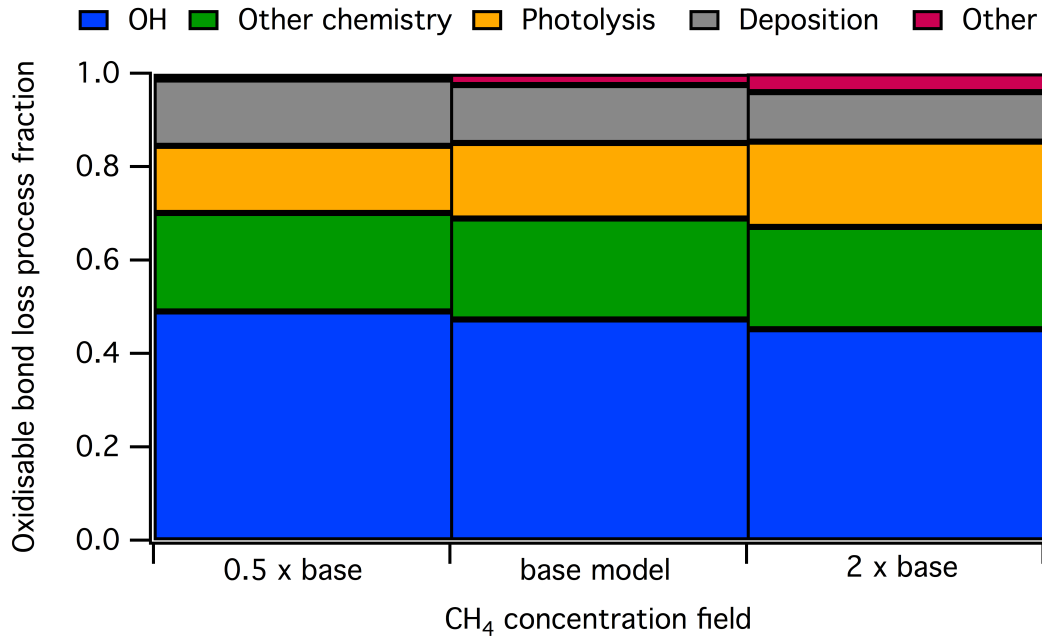


Figure 8. Oxidisable bond loss mechanism fractions under changing effective CH<sub>4</sub> emissions (0.5 x CH<sub>4</sub> concentration field, base simulation and 2 x CH<sub>4</sub> concentration field).

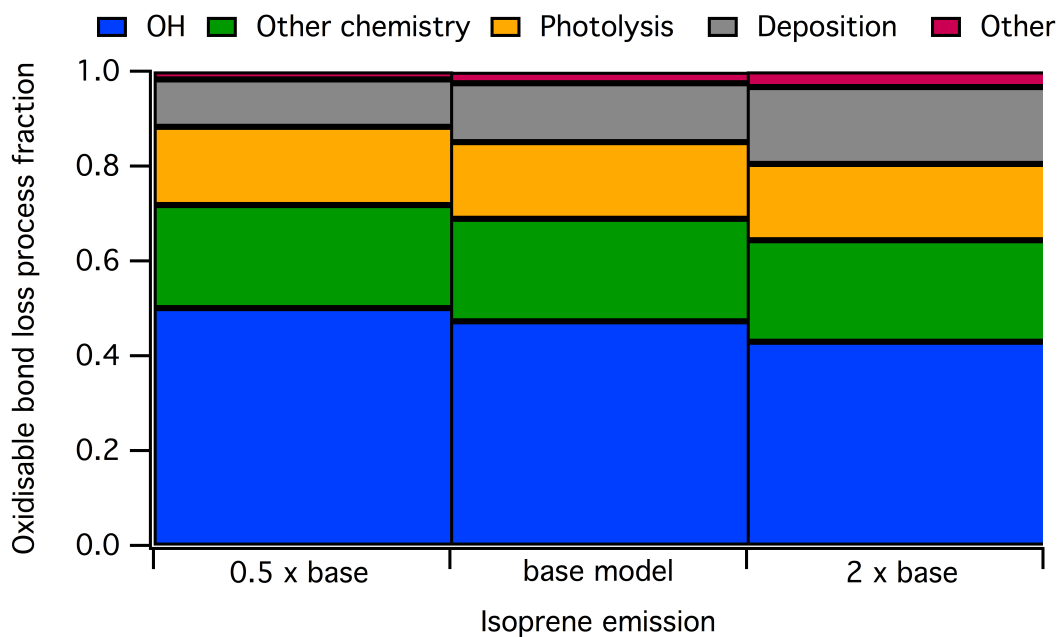


Figure 10. Oxidisable bond loss mechanism fractions under changing isoprene emissions.

- Supplement: The "errors in chemistry scheme" need some explanation, and these entries should be at the bottom of the table, as it doesn't aid the reader's comprehension to put them at the top.



We have added the following text to the supplement and moved the entries to the bottom of table S1.

Inconsistencies within the chemistry scheme, where the lumped nature of some reactions result in a non-physical production or loss of oxidisable bonds, are also tracked as errors in the chemistry scheme.

9. The supplement needs more detail on the implementation of the approach. It would be difficult for anyone to replicate in a different model without more information about the reaction classification. It would be helpful to provide a worked example of how the multiple in the Table is arrived at, and this could be included in the supplement.

The following has been added to the supplement.

Reaction tags were added to all reactions in the chemistry scheme, and the GEOS-Chem diagnostic was used to provide a direct measure of their production. An example of how this was implemented is shown below for a select few steps of the methane oxidation scheme illustrated in Fig. 1.



Reaction tags used in example reactions: Tag1 = Oxidisable bond lost via OH chemical reaction; Tag2 = Oxidisable bond + OH → 1 radical (RO<sub>2</sub>); Tag3 = OH + CH<sub>4</sub> reaction (special tag used to calculate effective CH<sub>4</sub> emission); Tag4 = RO<sub>2</sub> to peroxide; Tag5 = HO<sub>2</sub> to peroxide; Tag6 = RO<sub>2</sub> lost to carbonyl forming peroxy radical self reaction; Tag7 = Bond lost to RO<sub>2</sub> + RO<sub>2</sub> → 0 radicals.

Typos and minor issues

10. The English grammar needs a little work in places, particularly where the subject of a verb is inappropriate (e.g., "GEOS-Chem fixes CH<sub>4</sub> concentrations..." on line 318 would be clearer as "CH<sub>4</sub> concentrations are fixed in GEOS-Chem...")

This has been addressed.

11. I.133: add the before top

This has been addressed.

12. I.251: grammar in first sentence needs correcting.

This has been addressed.

13. I.358: MO<sub>2</sub> should be written as CH<sub>3</sub>O<sub>2</sub> for consistency with line 356, and it would be helpful to do this throughout the text, e.g., line 427/8.

This has been addressed.

14. Numbers less than 10 without units are better presented as text than numerals.

This stylistic change has not been implemented, but the authors are happy to do so if the editor wishes.

## Anonymous Referee #2

### *General Comments*

This paper presents a new method for diagnosing ozone production based on the processing of chemical bonds. The authors show that this new diagnostic changes our view of the relative importance of different hydrocarbon emissions, which is an improvement over previous methods using a simple total carbon-based approach. The authors also quantify the ozone-producing efficiency of the emitted bonds. The ability of this diagnostic to separate the difference between shifting the NO/NO<sub>2</sub> ratio and its impact on ozone production vs. the increase in the fraction of RO<sub>2</sub> reacting with NO is valuable. Overall, the discussion of the diagnostic and model sensitivities is quite lengthy and could be shortened by spending less time on the discussion of methane, per the comment below. This paper should be published after addressing the comments below, in particular, how this diagnostic could be relevant to our understanding of the differences in ozone production across models without actually implementing the diagnostic in every single chemical transport model.

### *Specific Comments*

15. The discussion of methane and isoprene is confusing due to the model implementation of methane as a fixed concentration. It might be better to focus the discussion on evaluating perturbations to isoprene emissions, and contrast that to methane, as opposed to the way it is presented now, with the caveat about model treatment of methane. Then the discussion of the dependence of methane 'emission' on OH would not be needed (i.e. Figure 7) which is difficult to follow.

We accept the reviewers comment that the discussion of methane and isoprene could be confusing. However, the fundamental differences in both their chemistries and treatment in the majority of chemical transport models mean we strongly feel that they warrant individual treatment. We have significantly shortened and simplified the discussion of methane, and have simplified Fig. 7 (see comment 6 above). As the 1<sup>st</sup> reviewer did not have an issue with the individual discussions of methane and isoprene we respectfully leave it to the editor to decide if our response to this comment is adequate.

16. This analysis would also be strengthened by presenting the types of information that global model comparisons of ozone production should include to take advantage of this type of diagnostic. For example, it seems that if all models presented their total methane, isoprene, CO, and NO<sub>x</sub> budgets, this diagnostic would help interpret the resulting impact on ozone production without actually implementing the diagnostic in each model. This might increase the scientific contribution of this paper.

We have added the following paragraph to the conclusions section of the paper.

Another potentially important application is in model-model comparisons. Increases in our understanding of why different models calculate different O<sub>3</sub> production and burdens has been slow [Stevenson *et al.*, 2006; Wu *et al.*, 2007; Young *et al.*, 2013]. Although a complete tagging like that described here is unlikely to occur for all of the models involved in the comparison, a small number of additional diagnostics is likely to produce a significantly better understanding of the models. Diagnosing (1) the total bond flux (direct emissions plus the flux for those species kept constant), (2) the rate of production of RO<sub>2</sub> and (3) the rate of production of O<sub>3</sub>, could help differentiate why certain models produce more or less O<sub>3</sub> than others. The ratios between these fluxes would help identify what aspect of the emissions of chemistry differs between the models.

17. The paragraph starting on line 341 needs clarification. What do you mean by “the final 20% due to the increased OH competing for the available oxidisable bonds.” Doesn’t this just mean that with higher NO<sub>x</sub>, you get higher OH concentrations and thus you increase the concentration of RO<sub>2</sub> as well and NO?

This sentence has been reworded to avoid confusion.

“the final 20% due to the increased OH concentration competing for the available oxidisable bonds and resulting in increased RO<sub>2</sub> production.”

*Technical Corrections*

18. Is discussing SO<sub>2</sub> oxidation relevant to ozone in any way? If not, it is confusing and should be removed.

Although SO<sub>2</sub> oxidation has minimal direct impact on O<sub>3</sub> production it is still a source of peroxy radicals that are central to this diagnostic approach ( $\text{SO}_2 + \text{OH} + \text{O}_2 \rightarrow \text{SO}_3 + \text{HO}_2$ ). We therefore would prefer to keep the sentence on SO<sub>2</sub> for completeness and also to aid others in reproducing the diagnostic approach.

19. You say that over a long enough timescale, the global atmosphere can be considered to be in steady-state, and thus equation (1) applies. Please clarify the conditions where this diagnostic is useful/applicable. For example, could it be used for a daily analysis of ozone production.

See response to comment 2.

20. Please be consistent with the use of CH<sub>3</sub>O<sub>2</sub> or MO<sub>2</sub>.

This has been addressed.

21. On line 438, the sentence that starts with “With the majority” is not a full sentence.

This has been addressed.

22. On line 440, remove the comma after OH.

This has been addressed.

# A new diagnostic for tropospheric ozone production

Peter M. Edwards<sup>1\*</sup> & Mathew J. Evans<sup>1,2</sup>

<sup>1</sup> Wolfson Atmospheric Chemistry Laboratories, Department of Chemistry, University of York, Heslington, York, YO10 5DD, UK

<sup>2</sup> National Centre for Atmospheric Science, Department of Chemistry, University of York, Heslington, York, YO10 5DD, UK

[\\*pete.edwards@york.ac.uk](mailto:pete.edwards@york.ac.uk)

## Abstract

Tropospheric ozone is important for the Earth's climate and air quality. It is produced during the oxidation of organics in the presence of nitrogen oxides. Due to the range of organic species emitted and the chain like nature of their oxidation, this chemistry is complex and understanding the role of different processes (emission, deposition, chemistry) is difficult. We demonstrate a new methodology for diagnosing ozone production based on the processing of bonds contained within emitted molecules, the fate of which is determined by the conservation of spin of the bonding electrons. Using this methodology to diagnose ozone production in the GEOS-Chem chemical transport model, we demonstrate its advantages over the standard diagnostic. We show that the number of bonds emitted, their chemistry and lifetime, and feedbacks on OH are all important in determining the ozone production within the model and its sensitivity to changes. This insight may allow future model-model comparisons to better identify the root causes of model differences.

## 1. Introduction

The chemistry of the troposphere is one of oxidation [Levy, 1973; Kroll *et al.*, 2011]. Organic compounds together with nitrogen and sulfur containing molecules are emitted into the troposphere where they are oxidised into compounds which can either be: absorbed by the biosphere; are involatile enough to form aerosols; can deposit to the surface; or be taken up by clouds and rained out. The oxidation of these compounds is significantly slower than might be expected based on the atmospheric composition of 20% molecular oxygen (O<sub>2</sub>).

31 The inefficiency of ground state O<sub>2</sub> as an atmospheric oxidant is due to its electronic  
32 structure. In quantum mechanics, all atomic particles have an intrinsic angular  
33 momentum known as spin [Atkins and De Paula, 2014]. The spin of an electron is  
34 described by the spin quantum number, s, and can have values of either +½ or -½ for a  
35 single electron. The Pauli exclusion principle states that if two electrons occupy the  
36 same orbital then their spins must be paired, and thus cancel. With two unpaired  
37 electrons, ground state O<sub>2</sub> is a spin-triplet with a total spin quantum number S=½+½=1,  
38 (giving a term symbol of <sup>3</sup>Σ<sub>g</sub><sup>-</sup>). In contrast, virtually all trace chemicals emitted into  
39 the atmosphere contain only paired electrons and are thus spin-singlets (S=0). The  
40 quantum mechanical spin selection rule ΔS=0 means that allowed electronic  
41 transitions must not result in a change in electron spin. From a simplistic perspective  
42 (i.e. ignoring nuclear spin interactions, inter-system crossings, nuclear dipole effects  
43 etc.) this spin selection rule, means that the reaction of ground state O<sub>2</sub> with most  
44 emitted compounds is effectively spin forbidden. Electronically excited O<sub>2</sub> (<sup>1</sup>Δ<sub>g</sub> or  
45 <sup>1</sup>Σ<sub>g</sub><sup>+</sup>) is a spin singlet and is more reactive in the atmosphere but low concentrations  
46 limit its role [Larson and Marley, 1999]. Instead, atmospheric oxidation proceeds  
47 predominantly via reactions with spin-doublet oxygen-derived species (S=½), notably  
48 the hydroxyl (OH) and peroxy radicals (RO<sub>2</sub> = HO<sub>2</sub>, CH<sub>3</sub>O<sub>2</sub>, C<sub>2</sub>H<sub>5</sub>O<sub>2</sub>, etc.), or spin-  
49 singlet species (e.g. ozone (O<sub>3</sub>)).

50 One of the few spin-triplet species in the atmosphere other than O<sub>2</sub> is the ground state  
51 of atomic oxygen (O(<sup>3</sup>P)), which readily undergoes a spin allowed reaction with O<sub>2</sub> to  
52 produce the spin-singlet O<sub>3</sub> molecule. This spin allowed reaction is responsible for the  
53 creation of O<sub>3</sub> in both the stratosphere, where it forms the protective O<sub>3</sub> layer, and the  
54 troposphere. The ability of O<sub>3</sub> to oxidise other spin-singlet species makes it a powerful  
55 oxidant, and it is thus considered a pollutant with negative health effects. Sources of  
56 O(<sup>3</sup>P) within the troposphere are limited because solar photons at sufficiently short  
57 wavelengths to directly photolyse O<sub>2</sub> to O(<sup>3</sup>P) are essentially unavailable.

58 Aside from the photolysis of O<sub>3</sub> itself, the only other significant source of  
59 tropospheric O(<sup>3</sup>P) is the photolysis of nitrogen dioxide (NO<sub>2</sub>) [Crutzen, 1971].  
60 Nitrogen oxides are emitted into the troposphere as nitrogen oxide (NO), which can be  
61 oxidised to NO<sub>2</sub> by O<sub>3</sub> and other oxidants. A large thermodynamic energy barrier  
62 prevents oxidation of NO to NO<sub>2</sub> by the OH radical [Nguyen et al., 1998], and  
63 therefore NO oxidation occurs through reaction with either O<sub>3</sub> or RO<sub>2</sub>. In terms of O<sub>3</sub>

Pete Edwards 9/8/2017 15:47

Deleted:

Pete Edwards 9/8/2017 15:54

Deleted: it

Pete Edwards 9/8/2017 16:43

Deleted: (

Pete Edwards 9/8/2017 16:44

Deleted: ,

Pete Edwards 9/8/2017 15:55

Formatted: Subscript

Pete Edwards 9/8/2017 17:00

Deleted: the

Pete Edwards 9/8/2017 17:00

Deleted: ,

Pete Edwards 9/8/2017 16:59

Deleted: ΔS=0,

71 production, the oxidation of NO by O<sub>3</sub> forms a null cycle. Thus only the reaction of  
72 NO with RO<sub>2</sub> leads to a net production of O<sub>3</sub>.

73 Exploring the distribution, source and sinks of tropospheric O<sub>3</sub> is a central theme of  
74 atmospheric science. Chemical transport models (online and offline) are essential  
75 tools enabling this understanding but their validity needs to be continually assessed.  
76 Model-model comparison exercises are commonly performed to assess performance,  
77 and comparisons of modelled O<sub>3</sub> budgets traditionally form part of this assessment  
78 [Stevenson *et al.*, 2006; Wu *et al.*, 2007; Wild, 2007; Young *et al.*, 2013]. Ozone  
79 production is diagnosed from the flux of NO to NO<sub>2</sub> via reaction with each of the  
80 speciated RO<sub>2</sub> in the model's chemical schemes. This approach provides information  
81 on the relative importance of the different RO<sub>2</sub> in the fast NO + RO<sub>2</sub> reactions within  
82 the model, but gives very little detail on how the longer time scale model processes  
83 (emissions, chemistry, deposition) influence O<sub>3</sub> production. Thus exploring the  
84 reasons that models differ in their O<sub>3</sub> production is difficult and progress has been  
85 slow.

86 A new diagnostic framework that links large scale model drivers such as emission,  
87 chemistry, and deposition to O<sub>3</sub> production would allow an improved assessment of  
88 why model ozone budgets differ. We attempt to provide such a framework here.

## 89 **2. A new diagnostic framework.**

90 The rate of production of tropospheric O<sub>3</sub> is limited by the rate of oxidation of NO to  
91 NO<sub>2</sub>, which is in turn limited by the rate of production of peroxy radicals (RO<sub>2</sub>).  
92 Peroxy radicals form through association reactions of hydrogen (H) atoms or alkyl  
93 radicals (both spin-doublets, S=1/2) with O<sub>2</sub>, forming a highly reactive spin-doublet  
94 radical on an oxygen atom. This spin allowed reaction converts spin-triplet O<sub>2</sub> that  
95 cannot react with spin-singlet pollutants into a spin-doublet O<sub>2</sub> containing species that  
96 can. As such the formation of RO<sub>2</sub> is central to the atmosphere's oxidation capacity,  
97 and its production is limited by the rate of production of H atoms or alkyl radicals.  
98 Thus the maximum potential rate of tropospheric O<sub>3</sub> production is equal to the rate at  
99 which H atoms and alkyl radicals are produced.

100 Hydrogen atoms and alkyl radicals are predominantly produced via the spin allowed  
101 breaking of the spin-pairing between the two electrons in a C or H containing covalent  
102 bond (S=0), such as those in hydrocarbons. These spin-pairings can be broken in the

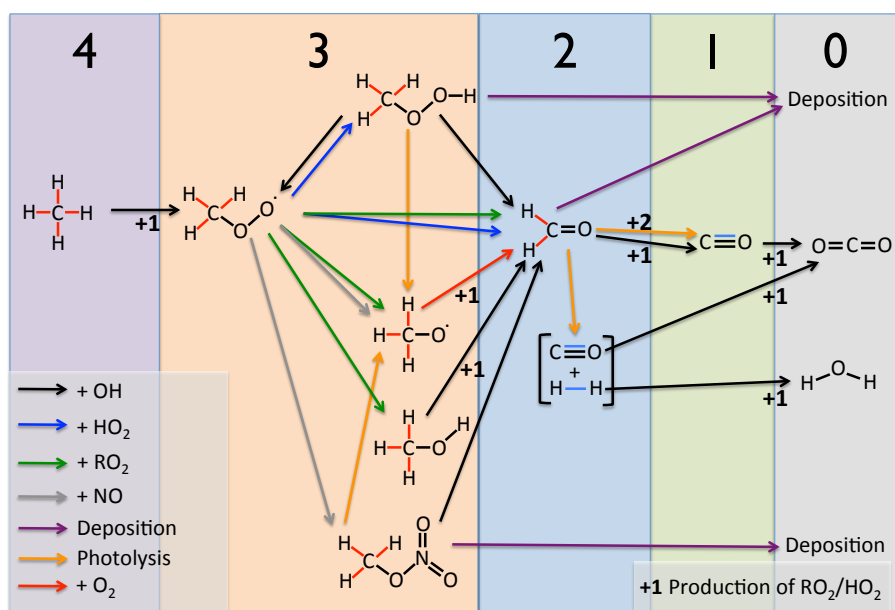
103 atmosphere either chemically or photolytically, with the products necessarily  
104 conserving spin. The breaking of a covalent bond by a photon ( $s=1$ ) can result in two  
105 products with  $S=1/2$  or two products with  $S=0$ . Likewise, oxidation by a radical ( $S = 1/2$ )  
106 will result in one product with  $S=0$  and one with  $S=1/2$ , because the unpaired electron  
107 on the radical reactant pairs with one of the covalent bond electrons to produce a spin-  
108 singlet.

109 Although the majority of  $RO_2$  is formed from emitted C or H containing covalent  
110 bonds, there are a few notable exceptions. Hydrogen atoms can also be produced  
111 through the oxidation of CO to  $CO_2$  by OH. During this reaction the coordinate bond  
112 between the C and O atom is broken and the H atom is produced via the breaking of  
113 the O-H bond. The other notable exception is the oxidation of an  $SO_2$  lone pair of  
114 electrons to  $SO_3$  by OH, where again the H atom produced comes from the OH. In  
115 both of these exceptions a spin-singlet electron pairing (CO coordinate bond or  $SO_2$   
116 lone pair) is broken during the production of the H atom, and we can therefore  
117 consider these reactions as similar to the breaking of C or H containing covalent bond.  
118 For simplicity these spin-singlet electron pairings that can be broken in the  
119 troposphere to produce either a H atom or alkyl radical will be referred to as  
120 “oxidisable bonds” (C-C, C-H, C=C, CO coordinate bond, S:).

121 Tropospheric  $O_3$  production occurs through the oxidation of NO by  $RO_2$ . Following  
122 the above rationale, these  $RO_2$  are produced during the spin allowed breaking of  
123 oxidisable bonds predominantly contained within emitted VOCs. This perspective  
124 allows us to build a new metric for the production of tropospheric  $O_3$  based around the  
125 spin conserving properties of oxidisable bond breaking. In the extreme case, all  
126 oxidisable bonds are photolysed to produce two spin-doublet  $RO_2$  products, which  
127 then react exclusively with NO to generate  $O_3$ . Thus at steady state, the maximum rate  
128 of  $O_3$  production is equal to the rate of production of  $RO_2$ , which is equal to twice the  
129 rate of destruction of the number of oxidisable bonds. This in turn is equal to twice the  
130 rate of emission of oxidisable bonds. Deviation from this maximum is determined by:

- 131 • The relative importance of processes that produce spin-singlet vs. spin-  
132 doublet products during oxidisable bond breaking;
- 133 • The fraction of spin-doublet products from oxidisable bond breaking which  
134 form  $RO_2$ ;
- 135 • The fraction of  $RO_2$  that go on to oxidize NO to  $NO_2$ .

136 To illustrate this Fig. 1 shows the tropospheric oxidation of a methane ( $\text{CH}_4$ ) molecule  
 137 through various steps to either a carbon dioxide ( $\text{CO}_2$ ) molecule or a species that is  
 138 deposited ( $\text{CH}_3\text{OOH}$ ,  $\text{CH}_2\text{O}$ ,  $\text{CH}_3\text{NO}_3$ ). Methane contains 4 x C-H oxidisable bonds  
 139 (8 paired bonding-electrons) and as the oxidation proceeds, the number of oxidisable  
 140 bonds decays to zero. Figure 1 highlights the steps in the tropospheric  $\text{CH}_4$  oxidation  
 141 mechanism that form spin-doublet products, with between 1 and 5  $\text{RO}_2$  produced  
 142 depending on the oxidation pathway. This compares with the theoretical maximum of  
 143 8 if all the original C-H bonds were photolysed to yield 2 spin-doublet products.



144  
 145 **Figure 1. Peroxy radical production during the tropospheric oxidation of  $\text{CH}_4$ .**  
 146 **Moving from left to right, the oxidisable bonds (emitted = red, produced = blue)**  
 147 **present in  $\text{CH}_4$  are removed via a range of tropospheric processes, indicated by**  
 148 **the coloured arrows. The large numbers across the top of the figure indicate the**  
 149 **number of oxidisable bonds at each stage of this oxidation. The production of**  
 150  **$\text{RO}_2$  is indicated by the +1/+2 numbers with the associated process arrows for**  
 151 **producing 1 or 2  $\text{RO}_2$  respectively.**

152 The principal atmospheric source of oxidisable bonds is the emission of C-H, C-C and  
 153 C=C bonds in hydrocarbons, with the only other significant sources being the  
 154 emission of CO and the chemical production of CO and  $\text{H}_2$  during hydrocarbon  
 155 oxidation. Over a long enough timescale, the global atmosphere can be considered to



156 be in a chemical steady state, where the rate of loss of oxidisable bonds is balanced by  
157 the rate of production or emission. Thus the  $O_3$  production rate can be described by  
158 equation (1), where the  $O_3$  production metric  $P_3O_3$  is equal to the number of spin-  
159 paired electrons in oxidisable bonds (i.e. twice the sum of the number of oxidisable  
160 bonds emitted ( $E_{bonds}$ ) and chemically produced ( $P_{bonds}$ )), multiplied by the number of  
161 spin-doublet radicals produced per oxidisable bond break divided by the maximum of  
162 2 ( $F_{Radicals}$ ), multiplied by the fraction of the radicals produced which are  $RO_2$  ( $F_{RO_2}$ ),  
163 multiplied by the fraction of  $RO_2$  that goes on to react with an  $NO$  to produce an  $O_3$   
164 molecule ( $F_{NO}$ ). A small correction ( $I$ ) for the production of  $RO_2$  via reactions of spin-  
165 doublet radicals other than those that result in the breaking of oxidisable spin-pairings  
166 (e.g.  $O_3 + OH \rightarrow HO_2 + O_2$ ) is included.

$$167 \quad P_3O_3 = \left( (2 \times (E_{bonds} + P_{bonds}) \times F_{radicals} \times F_{RO_2}) + I \right) \times F_{NO} \quad (1)$$

### 168 **3. Implementation**

169 We use the GEOS-Chem model to evaluate this new  $O_3$  production diagnostic. GEOS-  
170 Chem is a global chemical transport model of tropospheric chemistry, aerosol and  
171 transport ([www.geos-chem.org](http://www.geos-chem.org) version 9-02). The model is forced by assimilated  
172 meteorological and surface fields (GEOS-5) from NASA's Global Modelling and  
173 Assimilation Office, and was run at  $4^\circ \times 5^\circ$  spatial resolution. The model chemistry  
174 scheme includes  $O_X$ ,  $HO_X$ ,  $NO_X$ ,  $BrO_X$  and VOC chemistry as described in Mao et al.  
175 [2013] as are the emissions. The new  $P_3O_3$  diagnostic has been implemented via the  
176 tracking of reactions by type in the GEOS-Chem chemical mechanism file (further  
177 details given in the SI). This tracking of reactions enables the fate of all oxidisable  
178 bonds as well as the production and loss of all  $RO_2$  within the model to be determined  
179 using the standard GEOS-Chem production and loss diagnostic tools. Model  
180 simulations were run for 2 years (July 1<sup>st</sup> 2005 – July 1<sup>st</sup> 2007) with the first year used  
181 as a spin up and the diagnostics performed on the second year.

182 The standard GEOS-Chem diagnostic for  $O_3$  production ( $PO_3$ ) is shown on the left  
183 side of Table 1. This emphasizes the very fast cycling between  $NO$  and  $NO_2$ , but  
184 provides little in terms of higher process level information. The right side of Table 1  
185 shows the new budget for  $P_3O_3$ , which tracks the processing of oxidisable bonds  
186 within the model. Both diagnostic methods give the same final answer but our new  
187 methodology provides more process level detail. Figure 2 illustrates this new process

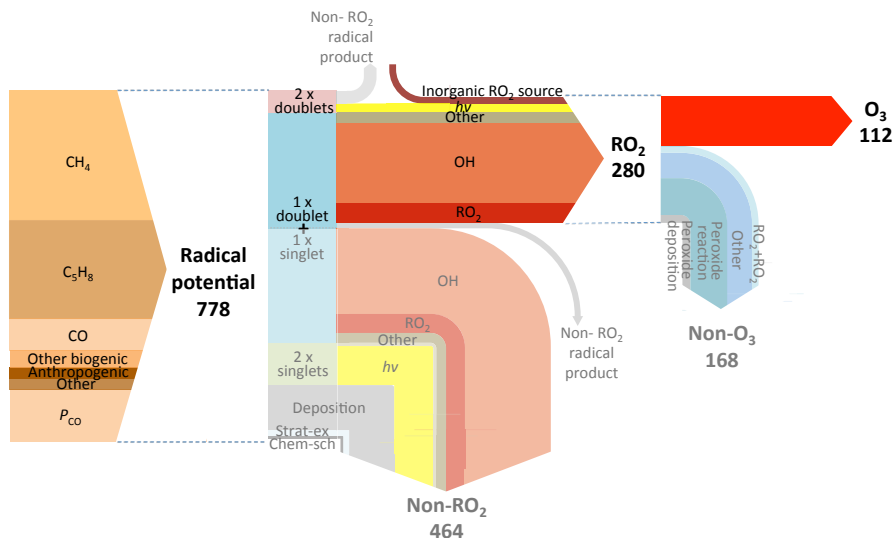
188 based approach, showing the flow of emitted oxidisable spin-paired electrons (bonds)  
 189 to O<sub>3</sub> and the magnitude of the various mechanisms that contribute to and compete  
 190 with O<sub>3</sub> production. The annual oxidisable bond emission of 389 T mol yr<sup>-1</sup> has the  
 191 potential to create 778 T mol yr<sup>-1</sup> of radicals. If all oxidisable bonds were broken by  
 192 photons to produce two radical products the RO<sub>2</sub> production would be 778 T mol yr<sup>-1</sup>.  
 193 If the oxidisable bonds were instead broken via radical reaction (e.g. OH) then RO<sub>2</sub>  
 194 production would be 389 T mol yr<sup>-1</sup>. The various oxidisable bond breaking / removal  
 195 pathways within the model result in the production of 280 T mol yr<sup>-1</sup> of RO<sub>2</sub>, with the  
 196 remainder largely producing stable spin singlet products.

197 Of the 280 T mol yr<sup>-1</sup> RO<sub>2</sub> produced, 112 T mol yr<sup>-1</sup> reacts with NO to produce O<sub>3</sub>.  
 198 The remainder is lost through the reaction or deposition of RO<sub>2</sub> reservoir species  
 199 (RO<sub>2y</sub>= RO<sub>2</sub> + peroxides + peroxy-acetyl nitrates). For example the production of  
 200 methylperoxide (CH<sub>3</sub>O<sub>2</sub> + HO<sub>2</sub> = CH<sub>3</sub>OOH) results in the loss of 2 RO<sub>2</sub>'s. However,  
 201 the reaction of methylperoxide with OH can re-release CH<sub>3</sub>O<sub>2</sub> (CH<sub>3</sub>OOH + OH =  
 202 CH<sub>3</sub>O<sub>2</sub> + H<sub>2</sub>O). Thus, the production of methylperoxide represents the loss of a HO<sub>2</sub>  
 203 and the movement of a CH<sub>3</sub>O<sub>2</sub> into a peroxide RO<sub>2y</sub> reservoir species. The deposition  
 204 of a peroxide molecule is thus the loss of a RO<sub>2y</sub> reservoir species. Notable in Fig. 2 is  
 205 that the role of PAN and nitrate removal of global RO<sub>2y</sub> is negligible, instead being  
 206 dominated by peroxide production and loss and the reaction of RO<sub>2</sub> with O<sub>3</sub>.

<i>PO</i> <sub>3</sub> / T mol Yr <sup>-1</sup>		<i>PO</i> <sub>3</sub> / T mol Yr <sup>-1</sup> (except <i>F</i> <sub>Radicals</sub> , <i>F</i> <sub>RO2</sub> , and <i>F</i> <sub>NO</sub> which are all unitless)	
NO + HO <sub>2</sub> → NO <sub>2</sub>	74	<i>E</i> <sub>bonds</sub>	330
NO + CH <sub>3</sub> O <sub>2</sub> → NO <sub>2</sub>	27	<i>P</i> <sub>bonds</sub>	58
Other RO <sub>2</sub> + NO → NO <sub>2</sub>	10	<i>F</i> <sub>radicals</sub>	0.40
Other	1	<i>F</i> <sub>RO2</sub>	0.86
		Inorganic RO <sub>2</sub> source	15
		<i>F</i> <sub>NO</sub>	0.40
<b><i>PO</i><sub>3</sub></b>	<b>112</b>	<b><i>P</i><sub>s</sub>O<sub>3</sub></b>	<b>112</b>

207 **Table 1. Comparison of ozone production diagnostics for GEOS-Chem base**  
 208 **simulation. Standard model *PO*<sub>3</sub> diagnostics (left column) show reactions**  
 209 **responsible for NO to NO<sub>2</sub> conversions but provide little process level**

210 information. The new P<sub>s</sub>O<sub>3</sub> (right) provides increased information on the  
 211 processes controlling O<sub>3</sub> production within the model.

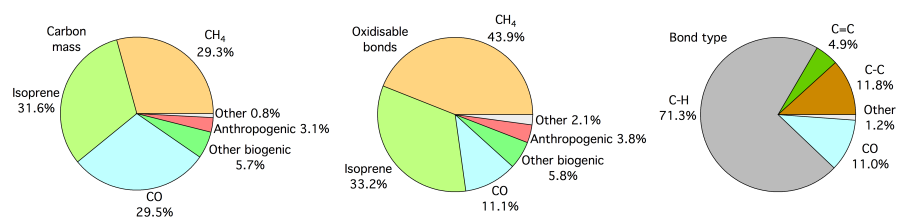


212  
 213 **Figure 2. Flow of oxidisable bonds to O<sub>3</sub> production in the GEOS-Chem base**  
 214 **simulation. Arrows are coloured according to process and the arrow thickness is**  
 215 **proportional to the flux through that channel. Spin-paired electrons are input as**  
 216 **oxidisable bonds into the model (left arrow), with the potential to create 778 T**  
 217 **mol yr<sup>-1</sup> of radicals. The actual fate of these bonds is shown in the central arrow,**  
 218 **producing 280 T mol yr<sup>-1</sup> of RO<sub>2</sub>, of which 112 T mol yr<sup>-1</sup> reacts with NO to**  
 219 **produce O<sub>3</sub> (right arrow).**

### 220 3.1 Emitted oxidisable bonds

221 The fuel for tropospheric oxidation chemistry is the emission of oxidisable bonds,  
 222 predominantly in the form of hydrocarbons. The production of tropospheric O<sub>3</sub> from  
 223 the spin-paired bonding electrons emitted into the standard GEOS-Chem model  
 224 occurs with an efficiency of 14% (112 T mol yr<sup>-1</sup> molecules of O<sub>3</sub> produced / 778 T  
 225 mol yr<sup>-1</sup> spin-paired electrons emitted as oxidisable bonds, Fig.2). These spin-paired  
 226 bonding electrons are predominantly emitted in the form of CH<sub>4</sub>, isoprene (C<sub>5</sub>H<sub>8</sub>) and  
 227 CO (37%, 28%, and 9% respectively). Oxidisable bonds produced during chemical  
 228 reactions (P<sub>bonds</sub>), account for 15% of the net source. Figure 3 shows emissions of CO  
 229 and hydrocarbons in the standard GEOS-Chem simulation in terms of mass of carbon  
 230 per compound, number of oxidisable bonds per compound and as number of bonds in

231 different oxidisable bond types. The commonly used carbon mass approach splits  
 232 emissions approximately equally between each of the major sources (CH<sub>4</sub> (29%),  
 233 Isoprene (32%) and CO (30%)). In contrast, the oxidisable bonds accounting approach  
 234 apportions hydrocarbon emissions 44%, 33% and 11% for CH<sub>4</sub>, isoprene and CO  
 235 respectively. This highlights the high number of oxidisable bonds per carbon atom in  
 236 CH<sub>4</sub> (4) compared to isoprene (2.8) and CO (1). Thus efforts to consider emissions on  
 237 a per-bond basis may provide more insight into chemical processes, as it is these  
 238 bonds that ultimately determine the chain-like chemistry rather than the mass of  
 239 carbon atoms. This helps to emphasise the relative importance of CH<sub>4</sub> emissions on  
 240 global tropospheric chemistry compared with other emissions such as isoprene or CO.  
 241 The type of oxidisable bond emitted is overwhelmingly C-H (71%).



242  
 243 **Figure 3. Pie charts showing hydrocarbon emissions in the base GEOS-Chem**  
 244 **simulation. Emissions split by carbon mass (left), number of oxidisable bonds**  
 245 **(centre) and bond type (right).**

246 The total emission and production of oxidisable bonds has the potential to create 778  
 247 T mol yr<sup>-1</sup> of radicals. However, only 6% of the oxidisable spin-pairings are broken to  
 248 give the maximum 2 spin-doublet products (e.g. radical channel of CH<sub>2</sub>O photolysis).  
 249 The majority (68%) are oxidized via reaction with a spin-doublet species (OH) to  
 250 produce 1 spin-singlet and 1 spin-doublet product (e.g. OH + VOC). The remaining  
 251 26% of spin-paired electrons are removed to form two spin-singlets (e.g. the non-  
 252 radical channel of CH<sub>2</sub>O photolysis). Thus, of the 778 Tmol yr<sup>-1</sup> spin-paired electrons  
 253 emitted or produced only 265 T mol yr<sup>-1</sup> (34%) are converted into RO<sub>2</sub>, with an  
 254 additional 15 T mol yr<sup>-1</sup> produced from reactions such as O<sub>3</sub> + OH → HO<sub>2</sub> + O<sub>2</sub> (*I*).  
 255 The efficiency of O<sub>3</sub> production from the available oxidisable bonds is further reduced  
 256 as only 40% of the 280 T mol yr<sup>-1</sup> of RO<sub>2</sub> produced react with NO to produce NO<sub>2</sub>.  
 257 The remainder is lost either through the self-reaction of RO<sub>2</sub> or via loss through  
 258 deposition or reaction of RO<sub>2y</sub> reservoir species (e.g. peroxides). Thus overall 14% of  
 259 the emitted bonding electrons go on to make O<sub>3</sub>.

260 The new O<sub>3</sub> production diagnostic presented here (*P<sub>s</sub>O<sub>3</sub>*) shows the impact of  
261 processes such as emission, deposition and chemical mechanism, and provides  
262 significantly more detail than the standard *PO<sub>3</sub>* diagnostic approach (Table 1). We  
263 now explore the sensitivity of model O<sub>3</sub> production to changing emissions of NO<sub>x</sub> and  
264 VOC from the perspective of the two diagnostic methods.

Pete Edwards 11/8/2017 10:42

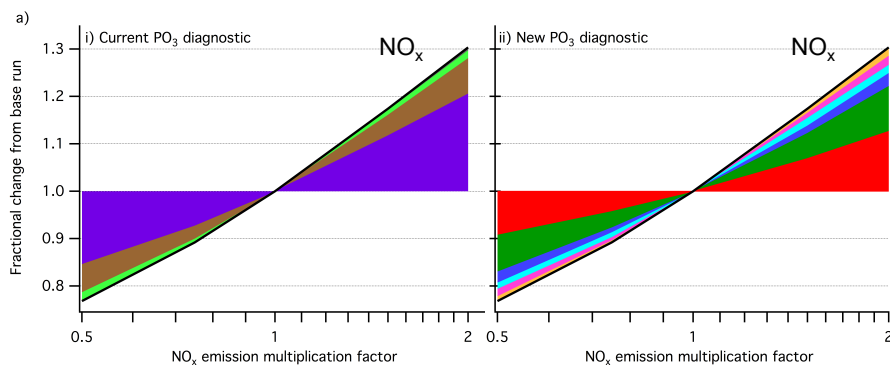
Deleted: is

Pete Edwards 11/8/2017 10:43

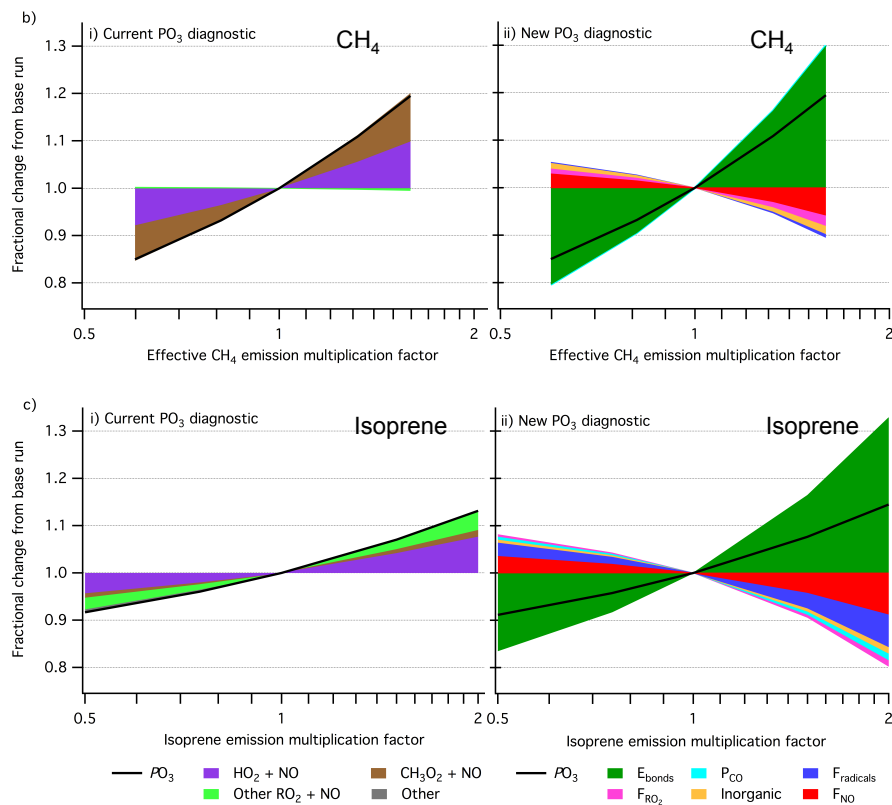
Deleted: ing

## 265 4 Model sensitivities

266 Understanding model response to changing emissions is an important tool for  
267 considering policy interventions. The major controls on O<sub>3</sub> production are emissions  
268 of NO<sub>x</sub> and VOCs. We show in Fig. 2 that from the perspective of global O<sub>3</sub>  
269 production, oxidisable bond emissions are dominated by CH<sub>4</sub> and isoprene. Figure 4  
270 shows the impact of changing emissions of NO<sub>x</sub>, isoprene and CH<sub>4</sub> on O<sub>3</sub> production  
271 from both the perspective of this new methodology and the conventional NO+RO<sub>2</sub>  
272 diagnostic approach. A set of 5 simulations was performed for each model sensitivity  
273 investigated (NO<sub>x</sub>, isoprene and CH<sub>4</sub>), with a common base simulation, resulting in 13  
274 simulations in total. The following sections investigate these model responses and use  
275 the new diagnostic to provide insight into the processes driving the observed response  
276 in O<sub>3</sub> production.



277



280

281

282 **Figure 4. Understanding the effect of  $\text{NO}_x$  and VOC emissions on ozone**  
 283 **production at the process level. Stack plots showing fractional change in model**  
 284  **$\text{PO}_3$  compared to base simulation and associated contributions from the current**  
 285  **$\text{PO}_3$  (i) and new  $\text{P}_5\text{O}_3$  (ii) diagnostic parameters under changing  $\text{NO}_x$  emissions**  
 286 **(a), effective  $\text{CH}_4$  emission (b) and isoprene emission (c). The  $\text{P}_5\text{O}_3$  diagnostic**  
 287 **parameters are derived for each model simulation using the diagnostic**  
 288 **implementation described in Sect. 3, and the fractional change in each parameter**  
 289 **from the base simulation calculated.**

290 **4.1  $\text{NO}_x$  emissions**

291 Figure 4a diagnoses the relative response of GEOS-Chem  $\text{O}_3$  production to changing  
 292  $\text{NO}_x$  emissions, using simulations where  $\text{NO}_x$  emissions from anthropogenic, biomass  
 293 burning, biofuels, soil and lighting sources were multiplied by factors of 0.5 - 2.  
 294 Increasing  $\text{NO}_x$  emissions increases  $\text{O}_3$  production. The standard  $\text{RO}_2+\text{NO}$  diagnostic  
 295 (Fig.4a(i)) shows that fractional contributions to the total change in  $\text{PO}_3$  from  $\text{HO}_2$

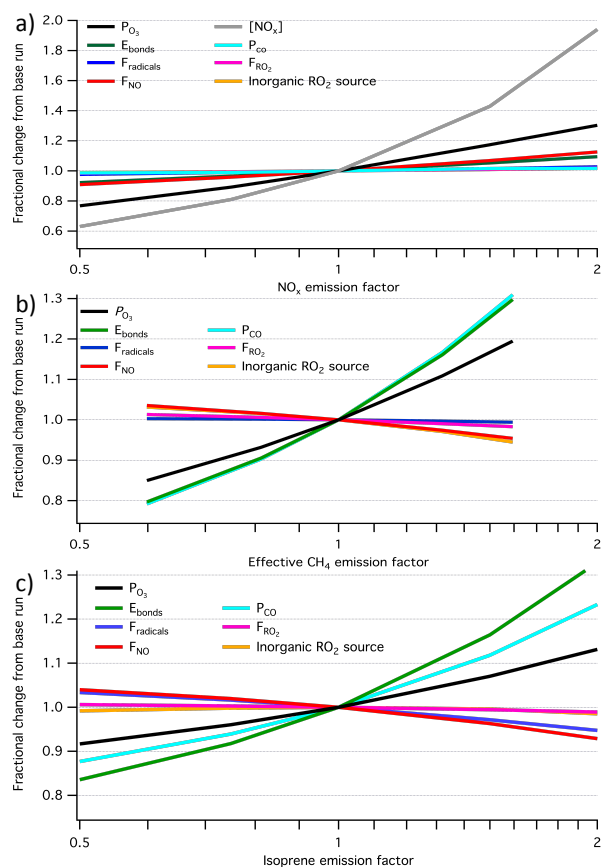
296 | (67%), methyl-peroxy ( $\text{CH}_3\text{O}_2$ ) (25%), and other  $\text{RO}_2$  (8%) remain approximately  
297 constant across the  $\text{NO}_x$  emission range investigated. This diagnostic provides little  
298 detail on the processes driving the change in  $\text{O}_3$  production under changing  $\text{NO}_x$   
299 emissions. In contrast, Fig. 4a(ii) is based on the new  $P_s\text{O}_3$  diagnostic and shows a  
300 range of process level changes occurring as  $\text{NO}_x$  emissions change.

#### 301 4.1.1 Impact of changing $\text{NO}_x$ emission on $F_{\text{NO}}$

302 Unsurprisingly, as  $\text{NO}_x$  emissions increase the fraction of  $\text{RO}_2$  reacting with  $\text{NO}$  to  
303 produce  $\text{NO}_2$  ( $F_{\text{NO}}$ ) increases (red section in Fig. 4a(ii)). However, this impact only  
304 accounts for around 40% of the increase in  $P_s\text{O}_3$ . Figure 5a shows the fractional  
305 change in all the  $P_s\text{O}_3$  efficiency parameters and the global mean  $\text{NO}_x$  concentration  
306 as a function of the changing  $\text{NO}_x$  emission. As  $\text{NO}_x$  emissions increase the increase  
307 in  $\text{NO}_x$  concentration in the model is somewhat dampened. Halving the  $\text{NO}_x$  emission  
308 leads to  $\text{NO}_x$  burdens dropping by ~35%, and doubling leads to an increase of 95%.  
309 This dampening is due to the impact of  $\text{NO}_x$  emissions on  $\text{OH}$  (see section 4.1.2),  
310 which is the dominant sink for  $\text{NO}_x$ . Increasing  $\text{NO}_x$  increases  $\text{OH}$  concentrations,  
311 which in turn shortens the  $\text{NO}_x$  lifetime thus dampening the response of concentration  
312 to emission.

Pete Edwards 11/8/2017 10:03

Deleted: M



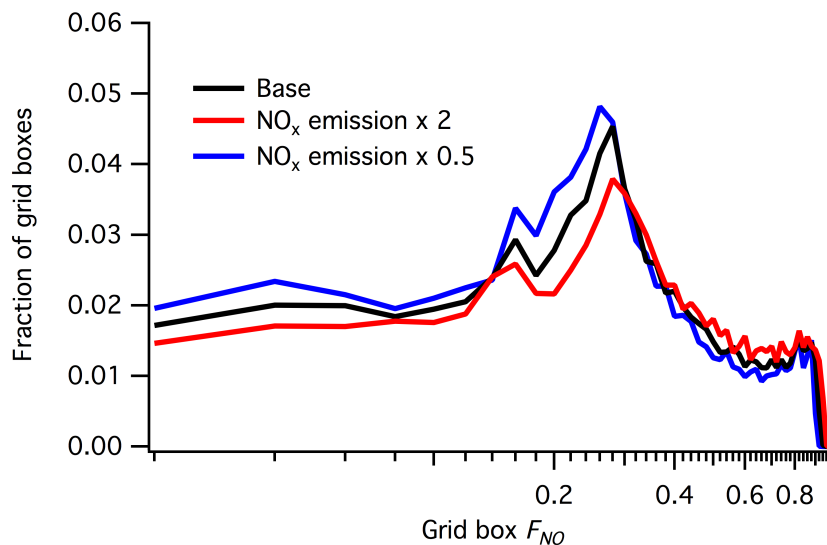
314

315 **Figure 5. Fractional change in new  $P_{O_3}$  diagnostic parameters from base run**  
 316 **against changing  $NO_x$  emission (a); effective  $CH_4$  emission (b); and isoprene**  
 317 **emission (c).**

318 The response of  $F_{NO}$  to changes in  $NO_x$  emissions is also dampened relative to the  
 319 change in  $NO_x$  emissions. This is due to spatial variability in  $F_{NO}$ , which is not  
 320 affected uniformly by changing  $NO_x$  emissions. Figure 6 shows the probability  
 321 distribution of  $F_{NO}$  values across all model grid boxes for the base simulation and the  
 322 half and doubled  $NO_x$  emission simulations (black, blue and red lines respectively).  
 323 For example, in a grid-box in the continental boundary layer where  $RO_2$  reacts  
 324 overwhelmingly with  $NO$ , doubling the  $NO_x$  emission may move  $F_{NO}$  from 0.90 to  
 325 0.95 but it can't double it. Similarly, in the remote boundary layer where  $RO_2$  reacts  
 326 overwhelmingly with other  $RO_2$  doubling  $NO_x$  emissions may move  $F_{NO}$  from 0.3 to



327 0.4 but again it doesn't double. Thus the geographical spread of NO<sub>x</sub> chemistry limits  
 328 the change in F<sub>NO</sub> caused by changing NO<sub>x</sub> emissions. The spatial variability in the  
 329 new P<sub>s</sub>O<sub>3</sub> diagnostic parameters shows that this approach has significant potential in  
 330 the analysis of regional O<sub>3</sub> budgets as well as global.



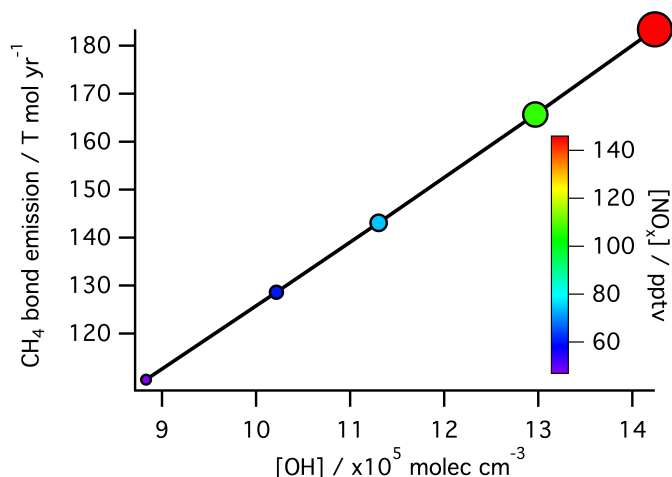
331  
 332 **Figure 6. Effect of NO<sub>x</sub> emission on distribution of F<sub>NO</sub> values (log scale).** F<sub>NO</sub>  
 333 values for each model grid box in the base and NO<sub>x</sub> emission x 0.5 and x 2  
 334 simulations, split into 50 x 0.02 width bins.

335 **4.1.2 Impact of changing NO<sub>x</sub> emission on E<sub>bonds</sub>**

336 Figure 4a(ii) shows that 60% of the response in P<sub>s</sub>O<sub>3</sub> to changing NO<sub>x</sub> emission is due  
 337 to factors other than F<sub>NO</sub>, with 40% of the increase due to changes in the emissions  
 338 (E<sub>bonds</sub>: 32%) and chemical production (P<sub>bonds</sub>: 8%) of oxidizable bonds. This increase  
 339 in E<sub>bonds</sub> is surprising given VOC emissions are unchanged in these simulations.  
 340 However, increasing NO<sub>x</sub> emissions results in an increased OH concentration in the  
 341 model, which then leads to an increase in CH<sub>4</sub> oxidation. Methane (CH<sub>4</sub>)  
 342 concentrations are fixed in GEOS-Chem, resulting in an increase in the effective CH<sub>4</sub>  
 343 emission, as OH concentrations increase, causing an increase in the total bond  
 344 emission (E<sub>bonds</sub>). Figure 7 shows the response of effective CH<sub>4</sub> bond emission to  
 345 global mean OH concentration as it changes with global mean NO<sub>x</sub> concentration,

Pete Edwards 11/8/2017 10:45  
~~Deleted: GEOS-Chem fixes~~  
 Pete Edwards 11/8/2017 10:46  
~~Deleted: s~~  
 Pete Edwards 10/8/2017 12:10  
~~Deleted: model~~  
 Pete Edwards 10/8/2017 12:10  
~~Deleted: and effective CH<sub>4</sub> bond emission as a function of~~  
 Pete Edwards 10/8/2017 12:10  
~~Deleted: across the simulations where the base NO<sub>x</sub> emissions are multiplied by factors from 0.5 to 2~~

354 More CH<sub>4</sub> oxidation also leads to more CH<sub>2</sub>O production and in turn more CO  
 355 production (P<sub>CO</sub>), accounting for a significant fraction of the increase in this term.

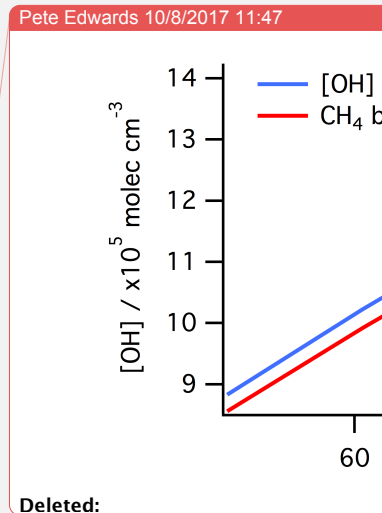


356  
 357 **Figure 7. Effective CH<sub>4</sub> emissions as a function of global mean OH concentration,**  
 358 **for simulations where NO<sub>x</sub> emissions were changed. Marker size and colour**  
 359 **indicate global NO<sub>x</sub> concentration.**

#### 360 4.1.3 Impact of changing NO<sub>x</sub> emission on F<sub>radicals</sub>, F<sub>RO2</sub> and I

361 The fraction of radicals produced from bond oxidation (F<sub>radicals</sub>) and the fraction of  
 362 those radicals which are RO<sub>2</sub> (F<sub>RO2</sub>) show slight positive increase with NO<sub>x</sub> emission,  
 363 accounting for 9% and 6% of the change in P<sub>s</sub>O<sub>3</sub> respectively. This reflects changes in  
 364 the partitioning of the fate of the oxidisable bonds, and is largely due to the changes in  
 365 OH. As OH increases with NO<sub>x</sub> emission, the rate of chemical oxidation of bonds  
 366 increases at the expense of other losses, in particular deposition. The inorganic RO<sub>2</sub>  
 367 source term (I) also correlates with NO<sub>x</sub> emission, as it is largely determined by the  
 368 concentrations of OH and O<sub>3</sub>. This change accounts for 5% of the observed change in  
 369 P<sub>s</sub>O<sub>3</sub>.

370 Thus, with this new diagnostic methodology it is evident that only 40% of the model  
 371 O<sub>3</sub> production response to changing NO<sub>x</sub> emission is due to the direct effect of  
 372 increasing NO concentration on the rate of RO<sub>2</sub> + NO reactions. Another 40% is due  
 373 to fixing the concentration of CH<sub>4</sub> within the model, with the final 20% due to the  
 374 increased OH concentration competing for the available oxidisable bonds and  
 375 resulting in increased RO<sub>2</sub> production.



Pete Edwards 10/8/2017 11:47  
 Deleted:  
 Unknown  
 Formatted: Font:(Default) Times New Roman, Bold, Font color: Custom Color(RGB(26,26,26))  
 Pete Edwards 10/8/2017 12:12  
 Deleted: Global mean OH concentration and e  
 Pete Edwards 10/8/2017 12:17  
 Deleted: Plot shows effective CH<sub>4</sub> emission tracks OH concentration in simulations where the NO<sub>x</sub> emission was increased or decreased from the base simulation. Note X-axis log scale.

## 384 4.2 Changing effective CH<sub>4</sub> emissions

385 As Fig. 2 shows CH<sub>4</sub> to be the largest single source of oxidisable bonds, this section  
386 investigates the response of the O<sub>3</sub> production diagnostics to changing CH<sub>4</sub> emissions.

387 Figure 4b shows the O<sub>3</sub> production diagnostics response to varying the CH<sub>4</sub> emission  
388 rate within the model. As the model uses prescribed CH<sub>4</sub> concentrations, these were  
389 varied by factors of between 0.5 and 2 from the base simulation, and the CH<sub>4</sub> emission  
390 diagnosed from the loss rate of CH<sub>4</sub> to reaction with OH, the only CH<sub>4</sub> loss in the  
391 model. We describe this as the effective CH<sub>4</sub> emission.

392 As effective CH<sub>4</sub> emission increases, O<sub>3</sub> production also increases. The standard  
393 diagnostic (Fig.4b(i)) shows that this increase occurs through an increased rate of  
394 reaction of HO<sub>2</sub> and CH<sub>3</sub>O<sub>2</sub> with NO, as would be expected as these are the RO<sub>2</sub>  
395 produced during CH<sub>4</sub> oxidation. The rate of other RO<sub>2</sub> + NO reactions actually  
396 decreases slightly as CH<sub>4</sub> emissions increase, due to lower OH concentrations and  
397 increased competition for NO from HO<sub>2</sub> and CH<sub>3</sub>O<sub>2</sub>. The new diagnostic (Fig.4b(ii)),  
398 however, shows the increase in O<sub>3</sub> production with increasing effective CH<sub>4</sub> emission  
399 is not simply a result of more HO<sub>2</sub> and CH<sub>3</sub>O<sub>2</sub>.

### 400 4.2.1 Impact of changing effective CH<sub>4</sub> emission on F<sub>NO</sub>

401 The observed change in P<sub>s</sub>O<sub>3</sub> is around one third smaller than would be expected from  
402 the increase in the oxidisable bond emission (E<sub>bonds</sub>) and bond production (P<sub>bonds</sub>)  
403 terms alone. This is due to a countering decrease in the other efficiency parameters  
404 with increasing effective CH<sub>4</sub> emission. Figure 5b shows the fractional change in all  
405 the efficiency parameters as a function of the changing effective CH<sub>4</sub> emission. The  
406 decrease in the fraction of RO<sub>2</sub> reacting with NO to produce NO<sub>2</sub> (F<sub>NO</sub>) is driven by  
407 increasing O<sub>3</sub> concentrations, which push the NO/NO<sub>2</sub> ratio towards NO<sub>2</sub>. This  
408 reduces the availability of NO to react with RO<sub>2</sub> thereby reducing O<sub>3</sub> production. This  
409 shift in the NO/NO<sub>2</sub> ratio also increases NO<sub>x</sub> loss within the model with increasing  
410 CH<sub>4</sub> emission, as the increased CH<sub>4</sub> oxidation increases RO<sub>2</sub> concentrations resulting  
411 in larger losses of NO<sub>2</sub> via compounds such as peroxyacetyl nitrate (PAN) and  
412 peroxyacetic acid (PNA).

### 413 4.2.2 Impact of changing effective CH<sub>4</sub> emission on E<sub>bonds</sub>

414 Increasing the effective CH<sub>4</sub> emission results in an increase in E<sub>bonds</sub>. Changing the  
415 fraction of total emitted oxidisable bonds from CH<sub>4</sub> does however have significant

Pete Edwards 10/8/2017 12:48

Deleted: effect on the

Pete Edwards 10/8/2017 12:49

Deleted: of

Pete Edwards 10/8/2017 12:36

Deleted: . The CH<sub>4</sub> emission rate (plotted) is

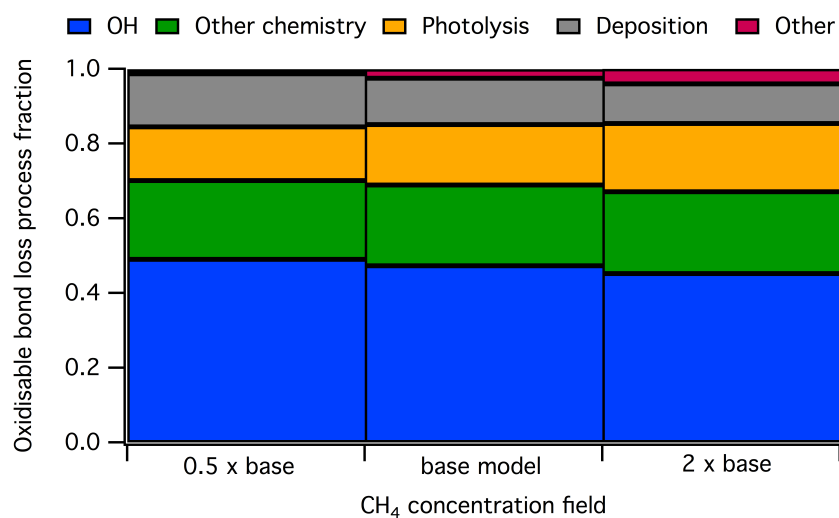
Pete Edwards 11/8/2017 10:03

Deleted: M

Pete Edwards 10/8/2017 14:49

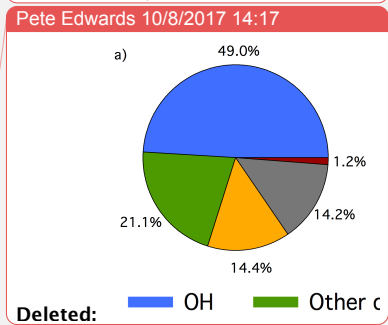
Deleted: As CH<sub>4</sub> is the largest single source of oxidisable bonds (Fig. 3), i

422 consequences on the loss mechanisms of these bonds, which influences the other  
 423 efficiency parameters. Figure 8 show the split of oxidisable bond loss mechanisms in  
 424 the base simulation and those with the CH<sub>4</sub> concentration fields multiplied by 0.5 and  
 425 2. As the effective CH<sub>4</sub> emission increases the fraction of bonds lost via OH  
 426 decreases, despite the actual number of oxidisable bonds lost to OH increasing. A  
 427 larger fraction of bonds are therefore lost via the other mechanisms shown in Fig. 8  
 428 rather than reaction with OH. As CH<sub>4</sub> removal occurs predominantly in the free  
 429 troposphere, increasing the effective CH<sub>4</sub> emission also results in a reduction in the  
 430 fraction of oxidisable bonds lost via deposition. The largest fractional increase in bond  
 431 loss mechanism with increasing effective CH<sub>4</sub> emission is for photolysis, with the  
 432 increase in the “other” fraction due to increased loss of bonds to the stratosphere with  
 433 increasing CH<sub>4</sub>.



Pete Edwards 10/8/2017 14:47  
 Deleted: The pie charts in  
 Pete Edwards 10/8/2017 14:47  
 Deleted: .

Pete Edwards 10/8/2017 14:48  
 Deleted: The fraction of bonds lost via other chemistry (e.g. non-OH radical oxidation and RO<sub>2</sub> self reactions) remains approximately constant across the effective CH<sub>4</sub> emission scenarios investigated.



Pete Edwards 10/8/2017 14:17  
 Deleted:  
 Unknown  
 Formatted: Font:(Default) Times New Roman

434  
 435 **Figure 8. Oxidisable bond loss mechanism fractions under changing effective**  
 436 **CH<sub>4</sub> emissions (0.5 x CH<sub>4</sub> concentration field, base simulation, and 2 x CH<sub>4</sub>**  
 437 **concentration field).**

438 **4.2.3 Impact of changing effective CH<sub>4</sub> emission on F<sub>radicals</sub>, F<sub>RO2</sub> and I**

439 The fraction of oxidisable bonds that goes on to produce radicals (F<sub>radicals</sub>) and the  
 440 fraction of these that are RO<sub>2</sub> (F<sub>RO2</sub>) also decrease with increasing effective CH<sub>4</sub>  
 441 emissions. This is due to decreasing global OH concentration resulting from increased  
 442 loss by reaction with CH<sub>4</sub> and a decreasing NO concentration. This favours bond loss

Pete Edwards 11/8/2017 12:05  
 Deleted: s  
 Pete Edwards 11/8/2017 12:06  
 Deleted: . Pie charts showing fractional loss mechanisms for oxidisable bonds in model simulations with  
 Pete Edwards 11/8/2017 12:06  
 Deleted:  
 Pete Edwards 10/8/2017 14:49  
 Deleted: (a)  
 Pete Edwards 10/8/2017 14:49  
 Deleted: (b)  
 Pete Edwards 10/8/2017 14:51  
 Deleted: —Page Break—

460 via pathways that produce less RO<sub>2</sub> (e.g. CH<sub>2</sub>O photolysis). The long lifetime of CH<sub>4</sub>  
461 compared with the majority of other sources of oxidisable bonds, also results in a  
462 decrease in the fraction of bonds lost to deposition as total bond oxidation increases  
463 fractionally in the free troposphere where deposition is a less significant loss  
464 mechanism than in the boundary layer.

### 465 4.3 Changing isoprene emission

466 The species through which the oxidisable bonds are emitted has a significant impact  
467 on O<sub>3</sub> production, due to their subsequent removal mechanisms. For example, in a  
468 simulation where the only emission of oxidisable bonds is CO, F<sub>radicals</sub> is 0.5 and F<sub>RO<sub>2</sub></sub>  
469 is 1 as the only CO sink is reaction with OH to produce one HO<sub>2</sub> (OH + CO → HO<sub>2</sub> +  
470 CO<sub>2</sub>). The CO coordinate bond, which in theory has the potential to produce 2  
471 radicals, only produces 1 radical, which is an RO<sub>2</sub>.

472 Isoprene has the most complex chemistry in the model and is the second largest  
473 source of bonds into the atmosphere after CH<sub>4</sub> (Fig. 3). Figure 4c shows the response  
474 of the two O<sub>3</sub> production diagnostics to varying the isoprene emission within the  
475 model. The standard diagnostic (Fig.4c(i)) shows that the most significant increase in  
476 P<sub>3</sub>O<sub>3</sub> from increasing isoprene emissions is from NO + HO<sub>2</sub> and non-CH<sub>3</sub>O<sub>2</sub> peroxy  
477 radicals, with a smaller increase from CH<sub>3</sub>O<sub>2</sub>. The new P<sub>3</sub>O<sub>3</sub> diagnostic (Fig.4c(ii))  
478 again provides more insight, showing significant offsetting of around a half between  
479 the terms.

#### 480 4.3.1 Impact of changing isoprene emission on F<sub>NO</sub>

481 The increased isoprene emission leads to a similar change in the magnitude of the  
482 total number of oxidisable bonds emitted (E<sub>bonds</sub>) as the simulations in which effective  
483 CH<sub>4</sub> emission were varied. However, the countering decrease in all of the efficiency  
484 parameters is much larger for isoprene than for CH<sub>4</sub>. Figure 5c shows the fractional  
485 change in the new P<sub>3</sub>O<sub>3</sub> ozone production diagnostic parameters as a function of  
486 isoprene emissions compared to the base simulation. The change in F<sub>NO</sub> is due to both  
487 a decrease in global mean NO<sub>x</sub> concentrations with increasing isoprene and the spatial  
488 distribution of isoprene emissions. The majority of global isoprene emissions are in  
489 regions with low NO<sub>x</sub> emissions, and thus low values of F<sub>NO</sub>. Figure 9 shows a  
490 decrease in global mean NO<sub>x</sub>, and global mean OH concentrations with increasing  
491 isoprene emissions, however, the effect is less than that seen when CH<sub>4</sub> is responsible

Pete Edwards 10/8/2017 15:01

Deleted: such as deposition rather than those that

Pete Edwards 10/8/2017 15:03

Deleted: is

Pete Edwards 10/8/2017 15:03

Formatted: Subscript

Pete Edwards 10/8/2017 14:54

Deleted: These changes are predominantly due to the chemistry of CH<sub>2</sub>O. As shown in Fig. 1, the oxidation of CH<sub>2</sub>O occurs either via reaction with OH or photolysis, with OH reaction yielding 1 RO<sub>2</sub> from the net breaking of 2 spin-singlet bonds, and the two photolysis channels yielding either 0 x RO<sub>2</sub> (spin-singlet products molecular channel) or 2 x RO<sub>2</sub> (spin-doublet products radical channel), with the molecular channel being dominant. The reduction in OH concentration with increasing CH<sub>4</sub> means photolysis increases its competition as a bond loss mechanism, which has the effect of reducing the average RO<sub>2</sub> production per CH<sub>2</sub>O oxidised. The increase in the fraction of total bonds lost through the CH<sub>2</sub>O photolysis as CH<sub>4</sub> increases thus results in a reduction in both F<sub>radicals</sub> and F<sub>RO<sub>2</sub></sub>. The reduction in F<sub>radicals</sub> due to changing CH<sub>2</sub>O fate, however, is largely offset by a reduction in the fraction of bonds lost via deposition as CH<sub>4</sub> increases.

Pete Edwards 10/8/2017 15:03

Deleted: is due to the

Pete Edwards 10/8/2017 15:04

Deleted: ing

Pete Edwards 10/8/2017 15:04

Deleted: increasing

Pete Edwards 11/8/2017 10:04

Deleted: M

Pete Edwards 11/8/2017 10:04

Deleted: MO<sub>2</sub>

Pete Edwards 11/8/2017 10:08

Deleted: With t

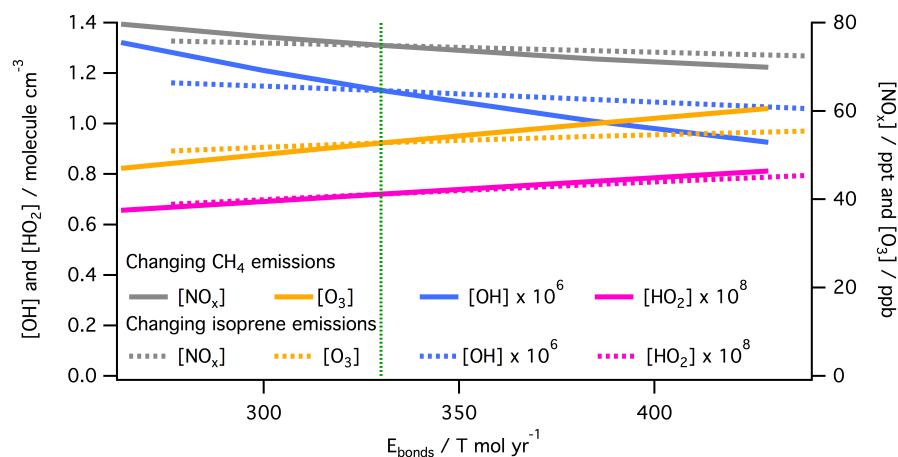
Pete Edwards 11/8/2017 10:08

Deleted: being

Pete Edwards 11/8/2017 10:08

Deleted: ,

525 for the same increase in oxidisable bond emission. This is due in a large part to the  
 526 spatial scales over which the two compounds impact.



527

528 **Figure 9. The effect of oxidisable bond parent species on OH, HO<sub>2</sub>, O<sub>3</sub> and NO<sub>x</sub>**  
 529 **concentrations. Global mean [OH], [HO<sub>2</sub>], [O<sub>3</sub>] and [NO<sub>x</sub>] for simulations where**  
 530 **the effective CH<sub>4</sub> emission (solid lines) and isoprene emission (dashed lines) were**  
 531 **changed, against model E<sub>bonds</sub>. The dashed vertical green line indicates E<sub>bonds</sub> in**  
 532 **the base simulation (330 T mol yr<sup>-1</sup>).**

533 **4.2.2 Impact of changing isoprene emission on E<sub>bonds</sub>**

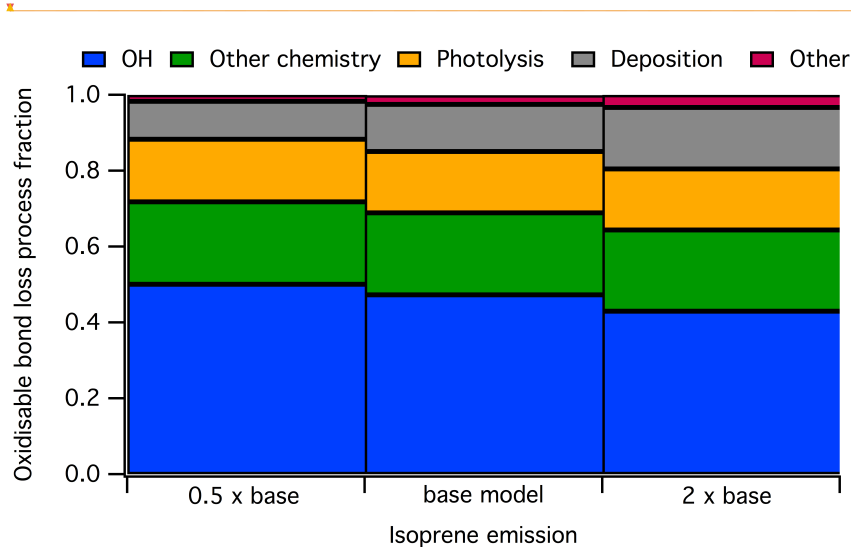
534 As isoprene is the second largest source of oxidisable bonds (Fig. 3), increasing the  
 535 isoprene emission results in a significant increase in E<sub>bonds</sub>. Differences in both the  
 536 spatial distribution of emissions and the oxidation chemistry of isoprene and CH<sub>4</sub>,  
 537 however, means that the impact of the increases in E<sub>bonds</sub> on O<sub>3</sub> production are  
 538 significantly different for the two compounds. This is predominantly because the  
 539 fraction of oxidisable bonds that are physically deposited for isoprene is high  
 540 compared to those emitted as CH<sub>4</sub>. This increase is due to i) the higher solubility of  
 541 isoprene oxidation products compared to those of CH<sub>4</sub>, and ii) the higher reactivity of  
 542 isoprene means its oxidation occurs in the boundary layer where both dry and wet  
 543 deposition is most effective.

544 | Figure 10 shows the fate of oxidisable bonds in the base simulation and those with the  
 545 isoprene emissions multiplied by 0.5 and 2. The complex myriad of products formed  
 546 during the isoprene oxidation mechanism also results in the production of many

Pete Edwards 10/8/2017 16:47  
 Deleted: split  
 Pete Edwards 10/8/2017 16:47  
 Deleted: loss mechanisms

549 highly oxygenated multifunctional compounds with high Henry's law solubility  
550 constants, meaning they are more readily lost to deposition.

551

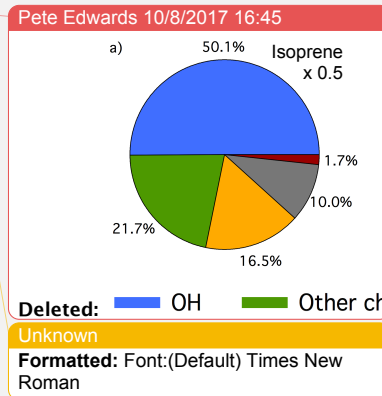


552

553 **Figure 10. Oxidisable bond loss mechanism fractions, under changing isoprene**  
554 **emissions.**

555 Increasing the isoprene emission also has a slight offsetting impact on the effective  
556 CH<sub>4</sub> emission, as increased isoprene concentrations decrease OH concentrations, and  
557 thus decrease the effective CH<sub>4</sub> emission. A doubling in isoprene emission causes a  
558 6% reduction in the effective emission of CH<sub>4</sub>.

559



Pete Edwards 11/8/2017 12:04

Deleted: s

Pete Edwards 10/8/2017 16:47

Deleted: Pie charts showing fractional loss mechanisms for oxidisable bonds in model simulations with 0.5 x isoprene emission (a), base simulation (b) and 2 x isoprene emission (c).

### 567 4.3.3 Impact of changing isoprene emission on $F_{\text{radicals}}$ , $F_{\text{RO}_2}$ and $I$

568 As shown in Fig. 3c(ii), increasing the isoprene emission results in a reduction in all  
569  $P_sO_3$  efficiency parameters. The reductions in  $F_{\text{radicals}}$  is due to the higher fraction of  
570 oxidisable bonds that are lost via non-radical forming pathways (e.g. deposition) for  
571 isoprene relative to the other main oxidisable bond emission sources  $CH_4$  and  $CO$ .  
572 The slight decreases of  $F_{\text{RO}_2}$  and  $I$  with increasing isoprene emission are  
573 predominantly due to changes in  $OH$  and  $NO_x$  (Fig. 9).

574 The complex chemistry of isoprene oxidation combined with the spatial distribution of  
575 isoprene emissions means the increase in  $O_3$  production due to increases in isoprene  
576 emissions is roughly half what might be expected from the increase in oxidisable bond  
577 emission alone (i.e. if the increase was *via*  $CO$  instead of isoprene).

## 578 5. Conclusions

579 We have shown that this bond-focussed approach to  $O_3$  production provides a  
580 significantly more detailed understanding of the processes involved. The role of  
581 modelled VOC emissions and  $O_3$  burden has been reported previously [Wild, 2007;  
582 Young *et al.*, 2013]. However previous efforts extending this to a general process led  
583 approach has not been successful. This new approach provides a tool with which the  
584 processes controlling  $O_3$  production can be investigated, and a metric by which  
585 different emissions can be compared. For example, the differing chemistry of isoprene  
586 and  $CH_4$  shows that even though their emissions of carbon mass are comparable, the  
587 atmosphere responds in different ways, with the isoprene bonds being less effective in  
588 producing  $O_3$  than  $CH_4$  bonds. By quantifying multiple steps in the  $O_3$  production  
589 process, competing changes in the system become apparent (as shown in Fig. 4b(ii)  
590 and c(ii)) and are thus testable. This enables the effect of model approximations on  $O_3$   
591 production to be quantified (e.g. the effect of  $NO_x$  on  $CH_4$  emissions when using  $CH_4$   
592 concentration fields).

593 This new diagnostic also points towards the importance of observational datasets for  
594 assessing our understanding of tropospheric chemistry. Although the budget presented  
595 in Fig. 2 provides an annually integrated global estimate it points towards local  
596 comparisons that can be made to assess model fidelity. Comparisons, both their  
597 magnitude and their ratios, between observed and modelled bond concentration, bond  
598 emission and loss fluxes (e.g.  $OH$  reactivity [Yang *et al.*, 2016] or depositional fluxes

Mat Evans 27/8/2017 07:37  
Moved (insertion) [1]



599 [\[Wesely and Hicks, 2000\]](#)), and O<sub>3</sub> production [[Cazorla and Brune, 2010](#)] would all  
600 provide comparisons for outputs from the P<sub>s</sub>O<sub>3</sub> diagnostic and help assess model  
601 performance.

602 Future work is necessary to identify the usefulness of this approach on smaller spatial  
603 and temporal scales. For regional modelling scale, the transport flux of bonds into the  
604 domain would need to be considered alongside the emissions of bonds. However, this  
605 might help to disentangle O<sub>3</sub> production due to local VOC emissions from that due to  
606 VOC emissions outside of the domain. This bond focussed approach may also have  
607 usefulness on shorter timescales. For example, when considering vertical fluxes in and  
608 out of the boundary layer, a bond centred approach could help. What fraction of the  
609 bonds emitted at the surface are exported to the free troposphere. If a measurement of  
610 reactivity flux could be made this could be tested experimentally.

611 ▲  
612 Another potentially important application is in model-model comparisons. Increases  
613 in our understanding of why different models calculate different O<sub>3</sub> production and  
614 burdens has been slow [[Stevenson et al., 2006](#); [Wu et al., 2007](#); [Young et al., 2013](#)].  
615 Although a complete tagging like that described here is unlikely to occur for all of the  
616 models involved in the comparison, a small number of additional diagnostics is likely  
617 to produce a significantly better understanding of the models. Diagnosing (1) the total  
618 bond flux (direct emissions plus the flux for those species kept constant), (2) the rate  
619 of production of RO<sub>2</sub> and (3) the rate of production of O<sub>3</sub> could help differentiate why  
620 certain models produce more or less O<sub>3</sub> than others. The ratios between these fluxes  
621 would help identify what aspect of the emissions of chemistry differs between the  
622 models.

Mat Evans 27/8/2017 07:38  
Deleted: -

Pete Edwards 28/8/2017 07:19  
Deleted: the

Mat Evans 27/8/2017 07:37  
**Moved up [1]:** This new diagnostic also points towards the importance of observational datasets for assessing our understanding of tropospheric chemistry. Although the budget presented in Fig. 2 provides an annually integrated global estimate it points towards local comparisons that can be made to assess model fidelity. Comparisons, both their magnitude and their ratios, between observed and modelled bond concentration, bond emission and loss fluxes (e.g. OH reactivity [[Yang et al., 2016](#)] or depositional fluxes [[Wesely and Hicks, 2000](#)]), and O<sub>3</sub> production [[Cazorla and Brune, 2010](#)] would all provide comparisons for outputs from the P<sub>s</sub>O<sub>3</sub> diagnostic and help assess model performance.

Mat Evans 27/8/2017 07:28  
Formatted: Subscript

Mat Evans 27/8/2017 07:28  
Formatted: Subscript

Mat Evans 27/8/2017 07:28  
Formatted: Subscript

Mat Evans 27/8/2017 07:30  
**Deleted:** A comparison between models based on this methodology may well help identify at a process level why models differ in their O<sub>3</sub> production. The application of this diagnostic to regional O<sub>3</sub> production should also increase insight into the processes controlling model O<sub>3</sub>.

648 **References**

- 649 Atkins, P. W., and J. De Paula (2014), *Atkins' Physical chemistry*, 10th ed., Oxford  
650 University Press.
- 651 Cazorla, M., and W. H. Brune (2010), Measurement of ozone production sensor,  
652 *Atmos. Meas. Tech.*, 3(3), 545–555, doi:10.5194/amt-3-545-2010.
- 653 Crutzen, P. J. (1971), Ozone production rates in an oxygen-hydrogen-nitrogen oxide  
654 atmosphere, *J. Geophys. Res.*, 76(30), 7311–7327,  
655 doi:10.1029/JC076i030p07311.
- 656 Kroll, J. H. et al. (2011), Carbon oxidation state as a metric for describing the  
657 chemistry of atmospheric organic aerosol., *Nat. Chem.*, 3(2), 133–139,  
658 doi:10.1038/nchem.948.
- 659 Larson, R. A., and K. A. Marley (1999), Singlet oxygen in the environment, *Environ.*  
660 *Photochem.*, 2, 123–136.
- 661 Levy, H. (1973), Photochemistry of minor constituents in the troposphere, *Planet.*  
662 *Space Sci.*, 21(4), 575–591, doi:10.1016/0032-0633(73)90071-8.
- 663 Mao, J., F. Paulot, D. J. Jacob, R. C. Cohen, J. D. Crouse, P. O. Wennberg, C. A.  
664 Keller, R. C. Hudman, M. P. Barkley, and L. W. Horowitz (2013), Ozone and  
665 organic nitrates over the eastern United States: Sensitivity to isoprene chemistry,  
666 *J. Geophys. Res. Atmos.*, 118(19), 1–13, doi:10.1002/jgrd.50817.
- 667 Nguyen, M. T., R. Sumathi, D. Sengupta, and J. Peeters (1998), Theoretical analysis  
668 of reactions related to the HNO<sub>2</sub> energy surface: OH + NO and H + NO<sub>2</sub>, *Chem.*  
669 *Phys.*, 230(1), 1–11, doi:10.1016/S0301-0104(97)00383-2.
- 670 Stevenson, D. S. et al. (2006), Multimodel ensemble simulations of present-day and  
671 near-future tropospheric ozone, *J. Geophys. Res. Atmos.*, 111(8),  
672 doi:10.1029/2005JD006338.
- 673 Wesely, M. L., and B. B. Hicks (2000), A review of the current status of knowledge  
674 on dry deposition, , 34.
- 675 Wild, O. (2007), Modelling the global tropospheric ozone budget: exploring the  
676 variability in current models, *Atmos. Chem. Phys.*, 7, 2643–2660,  
677 doi:10.5194/acpd-7-1995-2007.

678 Wu, S., L. J. Mickley, D. J. Jacob, J. A. Logan, R. M. Yantosca, and D. Rind (2007),  
679 Why are there large differences between models in global budgets of  
680 tropospheric ozone?, *J. Geophys. Res. Atmos.*, *112*(5), 1–18,  
681 doi:10.1029/2006JD007801.

682 Yang, Y., M. Shao, X. Wang, A. C. Nölscher, S. Kessel, A. Guenther, and J. Williams  
683 (2016), Towards a quantitative understanding of total OH reactivity: A review,  
684 *Atmos. Environ.*, *134*(2), doi:10.1016/j.atmosenv.2016.03.010.

685 Young, P. J. et al. (2013), Pre-industrial to end 21st century projections of  
686 tropospheric ozone from the Atmospheric Chemistry and Climate Model  
687 Biogeosciences Intercomparison Project (ACCMIP), *Atmos. Chem. Phys.*,  
688 *13*(10), 5277–5298, doi:10.5194/acp-13-5277-2013.

689

#### 690 **Author contributions**

691 All work presented here was conceived by P.M.E. and M.J.E. The implementation,  
692 model simulations and analysis were carried out by P.M.E., and the manuscript was  
693 written by P.M.E. with substantial input from M.J.E..

#### 694 **Additional information**

695 The authors declare no competing financial interests.

#### 696 **Acknowledgements**

697 P.M.E. was supported by NERC Grant NE/K004603/1. This work was also supported  
698 by the NERC funded BACCHUS project (NE/L01291X/1). GEOS-Chem  
699 ([www.geos-chem.org](http://www.geos-chem.org)) is a community effort and we wish to thank all involved in the  
700 development of the model.